35th Annual International Conference of the IEEE EMBS
Osaka, Japan, 3 - 7 July, 2013

Dynamic method of optical coherence elastography in determining viscoelasticity of polymers and tissues

Yue Wang, Nathan D. Shemonski, Steven G. Adie, Stephen A. Boppart, Michael F. Insana

Abstract — **In this paper, we report on a novel quantitative elastography technique that combines optical coherence tomography (OCT) with acoustic radiation force (ARF) excitation to estimate the complex modulus. Sinusoidally modulated ARF excitations between 200 – 4000 Hz generate a surface wave at the tissue surface that can be related to bulk viscoelastic (VE) properties in a manner that is both precise and quantitative. This method is very well suited to studying media at high spatial resolution and over a very broad range of force frequencies. Mechanical characterization was calibrated using hydropolymers before studying liver samples. Fresh porcine liver samples were measured over time with and without formalin fixation. These data were used to evaluate the utility of the Kelvin-Voigt rheological model commonly used to fit dispersion data when estimating modulus values. We also investigated use of square-wave force excitation to measure the step response of tissues.**

I. Introduction

Certain biomechanical properties of soft tissue, defined broadly as elasticity and viscosity, can have profound influences on pathological development in cancer. Mechanical properties are known to modulate the occurrence and severity of tumor fibrosis, cellular hyperplasia and other malignant behaviors [1]. Dynamic shear-wave elastography emerges as an efficient tool to quantitatively evaluate biomechanical properties without contacting tissues. By studying shear wave propagation, the mechanical visco-elasticity, anisotropy and nonlinearity properties are assessed. These properties have shown great potential as disease biomarkers. During the last decade, several shear-wave estimation techniques have emerged as tools for elasticity imaging and for measuring the complex shear modulus of tissues [2]-[6]. The advantage of using ARF to excite shear waves is its ability to explore a broad bandwidth of force excitation noninvasively in a spatially controllable manner.

OCT is capable of sensing displacements less than 1 μm with high spatial resolution and low system noise. Since shear and surface waves attenuate very quickly at high frequency (> 1 KHz), OCT is ideal for examining the mechanical response over the entire frequency range to detect which frequencies contain the most diagnostic information about the tissue pathology. However, the penetration depth of OCT sensors is very shallow, less than 2 mm, limiting the detection of body waves but not surface waves. Thus, we focus on accurately measuring surface wave speeds, which can be converted to shear-wave speeds [7]. In this paper, we demonstrate the feasibility of using ARF-based optical coherence elastography (OCE) to map the shear-wave speeds in biphasic polymer materials and mammalian liver tissue samples during fixation.

II. Material and Methods

A. US-OCT system setup

The optical source on the SD-OCT system was a 26 mW superluminescent diode (Praevium Research) with a center wavelength of 1330 nm and a bandwidth of 105 nm. The spectrometer used in our system (Bayspec, OCTS-1255-1330 -1405) included a 1024-pixel InGaAs linescan camera (Goodrich, LDH2), which was connected to a PC via a NI-IMAQ board (National Instruments, NI-PCIe 1427). Optical beam steering was achieved using an x-y galvanometer (SCANLAB, SCANcube 7) controlled by the PC via a multifunctional DAQ card (National Instruments, NI-PCIe 6353). The OCT system was operating in M-mode with the scan rate of 47 KHz. Details of the system setup can be found in Fig. 1. This system has a low numerical aperture (NA=0.03) to image a large range of depth, resulting in a FWHM transverse resolution around 20 μm. The axial resolution, however, was about 5 μm.

Ultrasound transducer (ValpeyFisher, Hopkinton MA, 8 MHz, 0.75-inch diameter, F-1) was fixed from the bottom. Tissue sample was placed on a thin agarose standoff pad mounted on a 3-D movable stage. A power amplifier (3100LA, 55dB, 250 KHz – 150 MHz) drove the US transducer to transmit ultrasound amplitude-modulated bursts. Radiation force was generated at the sample-air surface where the acoustic impedance changes dramatically. This radiation force was applied along the axial (z-axis) direction where the force magnitude was proportional to the acoustic intensity over a small area at the sample surface. Real-time feedback of the tissue motion allowed us to locate

*This work was supported in part by the Midwest Cancer Nanotechnology Training Center.

Y. Wang is with the Department of Bioengineering and Beckman Institute for Advanced Science and Technology, University of Illinois at Urbana-Champaign, Urbana, IL 61801, USA (e-mail: yuewang3@illinois.edu, phone: 217-333-0271).

N. D. Shemonski is with the Department of Electrical and Computer Engineering and Beckman Institute for Advanced Science and Technology, University of Illinois at Urbana-Champaign, Urbana, IL 61801, USA (e-mail: shemons1@illinois.edu).

S. G. Adie is with the Beckman Institute for Advanced Science and Technology, University of Illinois at Urbana-Champaign, Urbana, IL 61801, USA (e-mail: sgadie@illinois.edu).

S. A. Boppart and M. F. Insana are with Department of Bioengineering, Department of Electrical and Computer Engineering and Beckman Institute for Advanced Science and Technology, University of Illinois at Urbana-Champaign, Urbana, IL 61801, USA (e-mail: boppart@illinois.edu and mfi@illinois.edu).

978-1-4577-0216-7/13/$26.00 ©2013 European Union

the ultrasound focus precisely (see Figure 2(a)). This ARF was amplitude modulated at a sinusoidal frequency which generated a harmonic surface force at a specific frequency. The velocity of the surface wave was calculated by estimating the spatial-phase gradient of each shear wave over a range of transverse locations (Fig. 2(b)). Shear-wave speed in the bulk media is approximately 1.05 times surface wave speed [7]. Dispersion (change in shear speed with frequency) measurements were fit to values predicted from rheological models to find estimate the complex modulus.

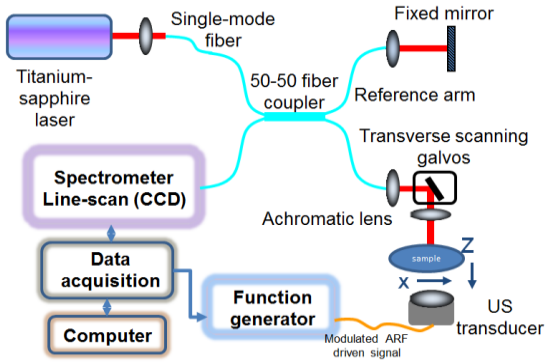

Fig. 1. The schematic of the system used for mechanical testing of soft tissue samples.

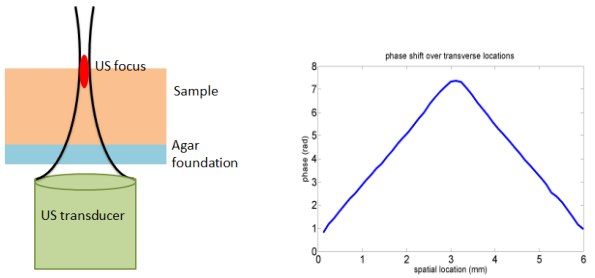

(a)

Fig. 2. (a) A focused ultrasound transducer generated surface waves at the sample surface. (b) Example of the phase shift measured over transverse locations in homogeneous media. The phase gradient was calculated through linear regression applied to the phase plot.

B. *Gelatin Phantom tests*

Gelatin gel samples (bi-phasic hydropolymers) at 4 and 8 percent concentrations were used in this study. Each cylindrical sample was 1-inch in diameter and 1 cm in thickness. Titanium dioxide particles were added to increase the optical contrast inside the gel. Details of phantom construction can be found in [5]. Three samples of each concentration were measured to test the repeatability of the technique.

OCT scan area was 6 x 6 mm containing 50 x 50 measurement points. Drive voltage of the ultrasound transducer was 16 V and 22 V for 4% and 8% gelatin sample, respectively. Voltage accounts for different strain responses observed for the two gel concentrations. Modulation frequency ranged from 200 Hz to 4000 Hz. Above 4000 Hz, the surface wave attenuated too quickly, resulting in noisy spatial-phase-gradient measurements.

C. *Porcine liver experiment*

Two liver samples were cut using a circular punch on freshly-excised porcine liver obtained from the Meat Lab, Department of Animal Science at University of Illinois. The liver was placed in iced saline (0.9% sodium chloride) immediately after harvesting and then transported to the lab for measurement. The diameter of samples was 1-inch and the thickness was approximately 1 cm. Prepared liver samples were warmed in saline at 23 °C for one hour before mechanical testing. One liver sample was monitored during the formalin fixation process. It was measured at four time points – 0 h, 20 min, 1 h, 2 h after soaking in 10% formalin in a 50 ml tube. The sample was washed in saline before making each measurement. A control sample was kept in saline between measurements made at 0 h, 40 min, 2 h.

The OCT scan area was 4 x 4 mm containing 50 x 50 measurement points. Drive voltage of the ultrasound transducer was between 34 - 40 V, where high voltages were used as samples stiffen during fixation. Modulation frequency ranged from 200 - 3500 Hz. Above 3500 Hz, the surface wave attenuated too quickly, resulting in noisy spatial-phase gradient measurements.

D. *Rheological models*

If a sample was purely elastic, it was also non-dispersive, and the relation between shear-wave speed and shear modulus is given by $c_s = \sqrt{\mu/\rho}$. Because all of the samples were dispersive, viscoelastic rheological models were implemented. Most commonly used is the Kelvin-Voigt viscoelastic model, where the complex shear modulus is expressed as $\mu(\omega) = \mu_1 + i\omega\eta$. μ_1 is the elastic modulus and η is the viscous modulus. The relation of shear wave speeds and two VE parameters is [4]

$$c_s(\omega) = \sqrt{\frac{2(\mu_1^2 + \omega^2\eta^2)}{\rho(\mu_1 + \sqrt{\mu_1^2 + \omega^2\eta^2})}} \quad (1)$$

Viscoelastic parameters μ_1 and η are estimated by least-squares fitting of the model to shear-wave speed measurements over the force-frequency bandwidth.

E. *Step excitation revealing relaxation frequency*

We also examined the step response of samples by replacing the harmonic modulated driving signal with a square-wave (in time) force excitation. At the ultrasonic focus, tissue exhibited an underdamped deformation response at the falling edge square-wave excitation (Fig. 3). This response was modeled as [9]

$$d(t) = \sum_{i=1}^{n} a_i e^{-\pi\gamma_i t}\cos(2\pi f_i t - \delta_i) + C \quad . \quad (2)$$

The natural vibration frequency of this underdamped oscillation was obtained for each sample by finding the central vibration frequency in the power spectrum of the response. We assumed the natural vibration frequency depends entirely on the mechanical constants of the sample

including local tissue mass.

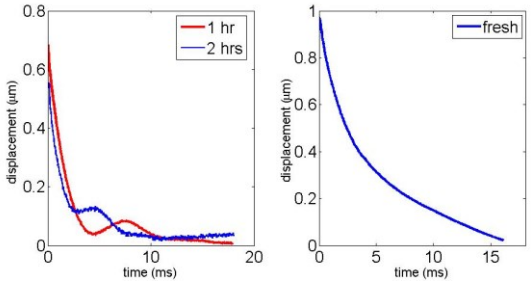

(a) (b)

Fig. 3. Optically measured displacement after turning off a step force. Plot (a) is from a liver sample following 1 hr and 2 hrs of formalin fixation. Plot (b) is the liver sample before fixation.

III. Results

A. Gelatin gel sample measurements

The shear-wave speeds estimated from six gelatin samples (three each at 8% and 4%) are shown in Fig. 4. Assuming an elastic, non-dispersive medium and selecting the shear-wave speed at 300 Hz, the shear modulus was found to be 2984.6 ± 130.2 Pa for 8% gelatin and 835.8 ± 86.5 Pa for 4% gelatin. Acknowledging dispersion and adopting a K-V viscoelastic model, the complex moduli estimated are presented in Table I. The natural vibration frequencies of the samples are also reported in the table. Errors represent the standard deviation based on three measurements.

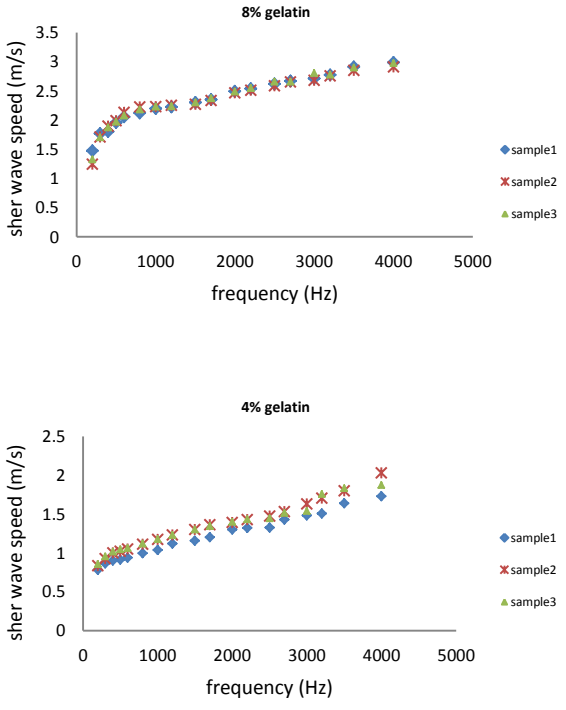

Fig. 4. Shear wave dispersion curves for three 8% and 4% gelatin gel samples.

TABLE I
Estimated Gelatin Viscoelastic Parameters

Gelatin concentration	μ1 [Pa]	η [Pa s]	f_n (step excite) [Hz]
4%	889.7±105	0.1±0.06	70.9±2.3
8%	3524.3±108	0.3±0.08	137.2±3.5

B. Shear modulus change of fresh liver during fixation

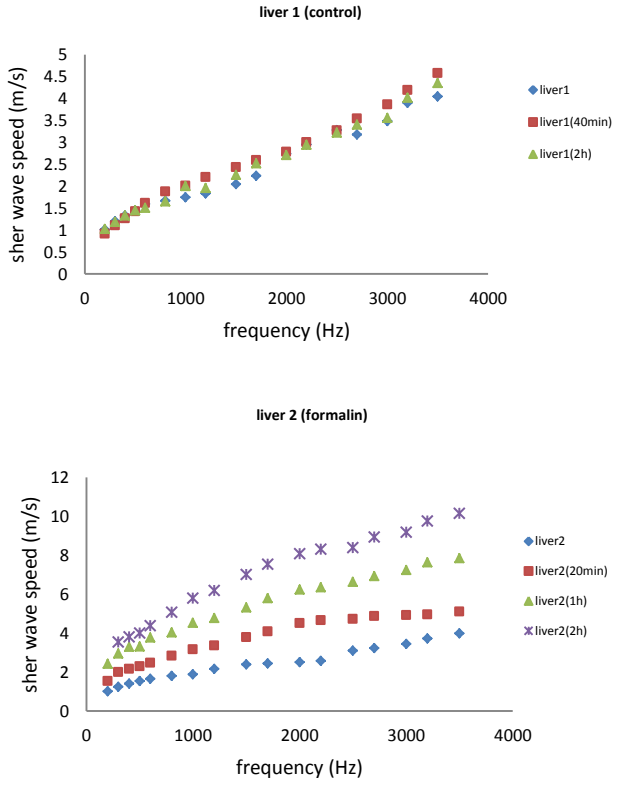

Fig. 5. Shear-wave dispersion curves in a control sample at three times (top) and a liver samples in formalin at three measurement times (bottom).

TABLE II
Estimated Liver Viscoelastic Parameters

Liver \ Time		0 min	20 min	40 min	1 h	2 h
1	μ1 [Pa]	1139.6	-	1098.2	-	1064.8
	η [Pa s]	0.37	-	0.41	-	0.40
2	μ1 [Pa]	1150.8	3475.7	-	8214.0	12108.8
	η [Pa s]	0.37	0.85	-	1.79	2.93

In Figure 5 and Table II, we presented details about mechanical property changes of the ex vivo liver sample during fixation in 10% formalin. Both elastic modulus and viscous modulus increased about 10 times after 2 hours fixation. Meanwhile, the control sample in saline showed little change over the 2 hour measurement time.

Step responses of the first measurement time point in liver 2 and all time points in liver 1 did not show obvious oscillatory behavior. (Figure 3(b)) The oscillation occurs only after fixation has occurred. The dominant oscillatory frequencies at 20 min, 1 h and 2 h fixation time points increases to, respectively, 127.3 Hz, 160 Hz, and 251.5 Hz. Mechanical resonance frequency of a simple spring-mass system is $\sqrt{k/m}$, where k is spring constant and m is the mass. This relationship holds in Table I because gelatin is a relatively elastic material. In highly viscous materials like fresh liver tissue, the oscillation magnitude is highly damped. The oscillatory behavior seen in Figure 3(a), after the liver has been fixed for two hours, occurs as chemical cross linking modifies the collagen structure to be more elastic in its behavior. AL, Oldenburg et al found similar change in the dominant vibrational frequency while fixing tissue, however, they had bulk vibration instead of local vibration, where former one depend much on the geometry of the sample. [11]

IV. Discussion

The purpose of this study is to provide measurement tools for studying mechanical properties of soft tissues over a broad force-frequency range. Many diseases such as cancer undergo biomechanical changes that can be seen at many spatial scales in tissue. It is believed that as force frequency increases, the mechanical resolution (which is determined by the shear wavelength) also increases. We successfully achieved reliable measurements of shear-wave speeds up to 4000 Hz. This could be increased further by using more focused ultrasound transducer and finer transverse sampling of the OCT scans. This technique shows great promise for investigating the force-frequency landscape of tissues.

Currently, we only considered one rheological model for all of the data regardless the resolution changes among the measurements. We have found that the Kelvin-Voigt model could provide very consistent estimates, although it doesn't represent all aspects of the dispersion measurements. The elasticity value predicted from the Kelvin-Voigt model increases 4 times when we double the gelatin concentration from 4% to 8%. This satisfies the rule that the modulus of the polymer increases quadratically with its concentration. The K-V model also successfully predict the elasticity increase while formalin fixing. One thing to note is that all Kelvin-Voigt predicted moduli in this paper show a large positive correlation between the elastic and viscous moduli. This finding might be an artifact of the model. Researchers have found [10] that the content of water, collagen, and the natural crosslinking do not change after formalin fixation, but the amount of methylene bridge (-CH_2-) cross-linking increases during fixation. These crosslinks increase the elasticity of the tissue as well as decrease the viscosity (resistance to fluid flow). The transition from overdamped to underdamped response also indicates a large increase in elasticity but not viscosity. However, the viscosity measured in Table II showed a 9-time increase in viscosity after 2 hours formalin fixation, which is most likely an artifact of the rheological model. Other viscoelastic models will be examined to more accurately predict the viscous modulus of the tissue, thus providing a more complete understanding of the tissue microstructure.

V. Conclusion

We measured the mechanical properties of tissues and polymers at force frequencies up to 4000 Hz using an ultrasonic radiation force excitation method with OCT particle motion tracking. Modulus values require the use of a rheological model, and the Kelvin-Voigt model yields reasonable measurements of the elastic modulus but not viscosity modulus estimates. Step responses are a promising alternative to harmonic-force excitation for measuring viscoelastic parameters locally. The preliminary data supports its usefulness in predicting the elasticity of "relatively elastic" materials. Alternative viscoelastic models are needed to describe the viscous behaviors.

Viscoelastic properties are important to quantify the tissue microenvironment that drives all inflammatory processes, especially cancers. The OCE method described in this paper has filled the void in our understanding of mechanical properties on the scale of a micrometer. It is expected to help illuminate the role of elastography in disease diagnosis.

Limitation of this technique lies in the optical penetrating depth. Although this method is developed mainly for imaging cell cultures and ex vivo tumors to explore basic science, clinic applications for example in eye and skin disease detections are still very promising.

References

[1] W.A.D. Anderson, *Pathology*. St Louis, MO: CV Mosby, 1953.

[2] S. Chen, M. Fatemi and J. F. Greenleaf, "Quantifying elasticity and viscosity from measurement of shear wave speed dispersion," *J Acoust Soc Am,* 115:2781-85, 2004.

[3] M. H. Kanai, "Propagation of vibration caused by electrical excitation in the normal human heart," *Ultrasound Med Biol*, 35:936-48, 2009.

[4] M. Orescanin, K. S. Toohey and M. F. Insana, "Material properties from acoustic radiation force step response," *J Acoust Soc Am*, 125(5):2928-36, 2009.

[5] M. Orescanin, M.A. Qayyum, K.S. Toohey, and M.F. Insana, "Dispersion and shear modulus measurements of porcine liver," Ultrason Imaging, 32(4):255-266, 2010.

[6] R. Sinkus, M. Tanter, T. Xydeas, S. Catheline, J. Bercoff, and M. Fink, "Viscoelastic shear properties of in vivo breast lesions measured by MR elastography," *Magnetic Resonance Imaging* ,2005. 23: 159-65.

[7] X. Zhang and J. F. Greenleaf, "Estimation of tissue's elasticity with surface wave speed," *J. Acoust. Soc. Am.* 122(5):2522-2525, 2007.

[8] M. Razani, A. Mariamplillai, C. Sun, T.W.H. Luk, V.X.D. Yang, M.C. Kolois, "Feasibility of optical coherence elastography measurements of shear wave propagation in homogeneous tissue equivaleng phantoms," *Biomed. Opt. Express,* 3(5): 972-980, 2012.

[9] V. Crecea, A.L. Oldenburg, X. Liang, T.S. Ralston, and S.A.Boppart, "Magnetomotive nanoparticle transducers for optical rheology of viscoelastic materials", *Optics Express*, 17(25):23114-23122, 2009.

[10] K. W. Fishbein, Y.A. Gluzband, M. Kaku, H. Ambia-Sobhan, S.A. Shapses, M. Yamauchi, R.G. Spencer, "Effects of formalin fixation and collagen cross-linking on T2 and magnetization transfer in bovine nasal cartilage," *Magn Reson Med*, 57(6):1000-1011, 2007.

[11] A. L. Oldenburg and S.A. Boppart, "Resonant acoustic spectroscopy of soft tissue using embedded magnetomotive nanotransducers and optical coherence tomography," *Phy Med Biol.* 55(4): 1189-1201, 2010.